ISSN 1063-7834, Physics of the Solid State, 2022. © Pleiades Publishing, Ltd., 2022.
Russian Text © The Author(s), 2022, published in Fundamental'nye Problemy Sovremennogo Materialovedeniya, 2022, Vol. 19, No. 2, pp. 205–212.

Investigation of the Structure and Properties of a Coating from a High-Entropy FeCoCrNiMn Alloy Obtained by a Wire Arc Additive Manufacturing

V. E. Gromov[a] (ORCID: 0000-0002-5147-5343), S. V. Konovalov[a, *] (ORCID: 0000-0003-4809-8660), Yu. F. Ivanov[a,b] (ORCID: 0000-0001-8022-7958), M. O. Efimov[a], I. A. Panchenko[a] (ORCID: 0000-0002-1631-9644), and S. V. Vorob'ev[a] (ORCID: 0000-0003-3957-0249)

[a] *Siberian State Industrial University, Novokuznetsk, 654007 Russia*

[b] *Institute of High Current Electronics, Siberian Branch, Russian Academy of Sciences, Tomsk, 634055 Russia*

**e-mail: konovalov@sibsiu.ru*

Received April 12, 2022; revised April 12, 2022; accepted April 28, 2022

Abstract—A coating of high-entropy Cantor alloy FeCoCrNiMn of nonequiatomic composition was formed on a 5083 aluminum alloy substrate by wire-arc additive manufacturing (WAAM). The methods of physical materials science were applied to analyze the structure, elemental composition, microhardness, and wear resistance of the coating–substrate system. The deposition of the FeCoCrNiMn high-entropy coating on the 5083 alloy surface is accompanied by the formation of microhardness and elemental composition gradients. Microcracks and micropores were revealed in the cross section of the coating. Microhardness in the volume of the coating is 2.5–3.5 GPa and increases to 9.9 GPa at the boundary with the substrate. In the middle part of the coating, the wear factor is 2.3×10^{-4} mm^3/N m; the friction coefficient is 0.7. A transition layer up to 450 μm thick is formed at the interface between the coating and the substrate. We analyzed the elemental composition gradient of the transition layer and noted a high level of chemical homogeneity of the coating. The found doping of the coating with substrate elements (aluminum) leads to the formation of a FeCoCrNiMnAl high-entropy coating, causing a lamellar structure at the interface between the transition layer and the substrate.

Keywords: FeCoCrNiMn high-entropy Kantor alloy, coating, substrate, 5083 aluminum alloy, mechanical properties, tribological properties, structure

DOI: 10.1134/S1063783422070034

INTRODUCTION

In the last two decades, the attention of researchers in the field of physical materials science has been drawn to the study of high-entropy alloys (HEAs). Articles, analytical reviews, and monographs consider the original results in the field of HEAs in detail, discuss the microstructure, properties, and thermodynamics of HEAs, assess the methods for simulating HEA structure, and offer new methods for obtaining multicomponent alloys [1–8]. Earlier, George et al. [1] and ourselves [5, 6] showed that nanostructures and even amorphous structures can be formed due to various methods for obtaining HEAs containing chemical elements with different atomic radii. One of the first high-entropy alloys under study is the FeCoCrNiMn alloy, which can maintain a face-centered cubic structure in a wide temperature range and has a good balance of strength and ductility [9]. Gludovatz et al. [10] showed that this alloy simultaneously demonstrates an increase in strength at room temperature and viscosity at cryogenic temperature (77 K) because of the dominance of twinning as a deformation mechanism.

One of the aspects of technical progress is the development and application of new HEAs with high mechanical, cryo- and heat-resistant, corrosion-resistant, special magnetic and electrical properties, as well as their compounds (carbides, nitrides, oxides, borides, silicides) [11, 12]. The fields of application of nitride HEA coatings [12] are rather wide, including biomedicine. They have a low modulus of elasticity, high chemical stability, wear and corrosion resistance in physiological media, low friction coefficient, biocompatibility, and excellent adhesion to the surface on which protective coatings are deposited.

The foregoing comments indicate the relevance and prospects of studying HEA coatings. This work analyzes the structure and properties of the FeCoCrNiMn Kantor HEA coating deposited on the 5083 alloy.

Table 1. Chemical composition of alloy 5083 (wt %)

Cr	Cu	Fe	Mg	Mn	Si	Ti	Zn	Other elements	Al
<0.25	<0.10	<0.40	4.0–4.9	<1.0	<0.10	<0.15	<0.25	<0.15	Rest

EXPERIMENTAL

Samples of the coating–substrate system were used as the objects of research. The coating was a high-entropy alloy of nonequiatomic elemental composition FeCoCrNiMn, formed on the substrate using the wire electric arc additive manufacturing (WAAM) [11, 13–15]. The substrate was an aluminum 5083 alloy (Table 1).

The structure and elemental composition of the coating and the substrate layer adjacent to the coating were studied by scanning electron microscopy (SEM) using an LEO EV50 microscope (Carl Zeiss) with an energy-dispersive analyzer. The properties of the coating and substrate were characterized by microhardness using an HV-1000 instrument at an indenter load of 0.5 N and wear resistance using a TRIBOtester instrument with factors: normal load 2 N, rotation speed 25 mm/s, friction path length 100 m, the radius of the friction track is 2 mm; the counterbody was a tungsten carbide ball with a diameter of 6 mm; tests were performed by dry friction in air at room temperature.

RESULTS AND DISCUSSION

The mechanical properties of the coating were studied by constructing a microhardness profile. The results showed that in the bulk of the coating, the microhardness values vary within 2.5–3.5 GPa (Fig. 1, region *1*) and increase to almost 10 GPa (9.91 GPa) at the boundary with the substrate (Fig. 1, region *2*). The hardness of the substrate at the boundary with the coating reaches 8 GPa and quickly (at a distance of 300 μm) decreases to 1.1 GPa, practically corresponding to the hardness of the substrate (1.0 GPa) (Fig. 1, region *3*). Tribological tests performed on the longitudinal section of the coating (section parallel to the coating/substrate interface) in its middle part showed that the wear factor of the coating is 2.3×10^{-4} mm^3/N m, and its friction coefficient is 0.7.

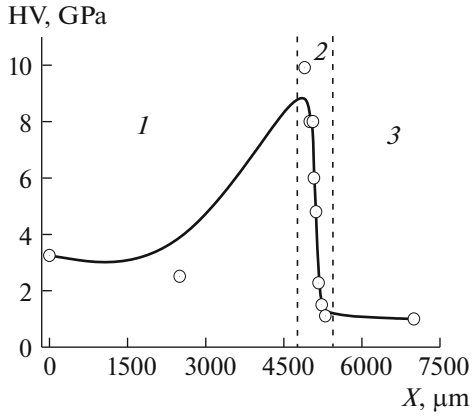

Fig. 1. Microhardness profile of the coating–substrate system: (*1*) coating, (*2*) transition layer, and (*3*) substrate.

The structure of the coating–substrate system was studied by scanning electron microscopy of an etched section (Fig. 2); three layers were revealed: the coating itself, the transition layer, and the substrate itself. The thickness of the transition layer varies quite significantly between 100 and 450 μm. The relatively extended transition layer corresponds to region 2 in Fig. 1 with high micro-hardness values.

The study of the cross section of the coating revealed micropores and microcracks. Depending on the degree of etching, the coating can be divided into three sublayers. The difference in the degree of etching indicates the inhomogeneity of the elemental composition of the coating.

The transition layer of the coating–substrate system has a highly developed relief, indicating that the coating has been fused into the surface layer of the substrate (Fig. 2a). There is a sublayer with an acicular (lamellar) structure between the transition layer and the substrate (Fig. 2b).

The results of X-ray microanalysis of the elemental composition of the upper region of the coating (Fig. 3) suggest that it contains not only the HEA components but also aluminum, a substrate element. The results of the quantitative analysis of the elemental composition of the upper and middle regions of the coating are given in Table 2.

The results obtained for the gradient of the elemental composition of the coating by X-ray microanalysis "by points" (Table 3) indicate a high level of chemical homogeneity of the coating. Significant concentration changes were revealed only for aluminum, which is an element of the substrate and got into the coating by diffusion during the formation of the coating–substrate system.

The results for the gradient of the elemental composition of the transition layer are shown in Fig. 4. Studies were carried out along two tracks located perpendicular to the surface of the coating. The thickness of the doped substrate layer reaches 450–500 μm. Alloying elements are distributed unevenly over the thickness of the substrate. For the track in Fig. 4a, the concentration of chemical elements that form the coating decreases with distance from the upper

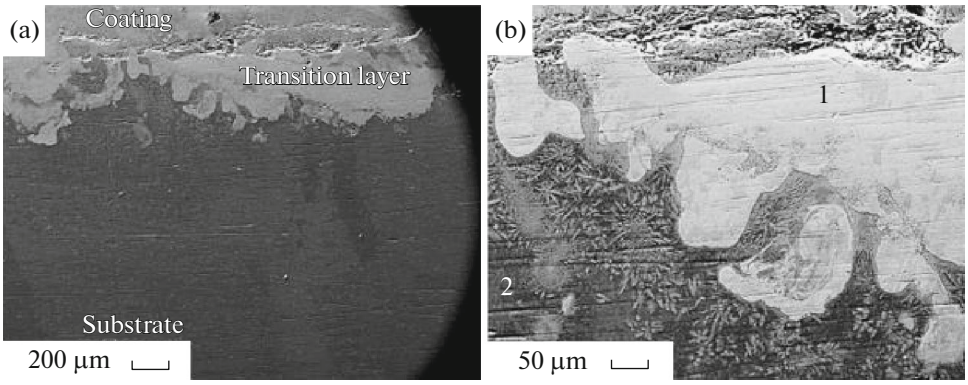

Fig. 2. (a) SEM images of the cross-sectional structure of the coating–substrate system; (b) (1) transition layer adjacent to the coating and (2) transition layer adjacent to the substrate.

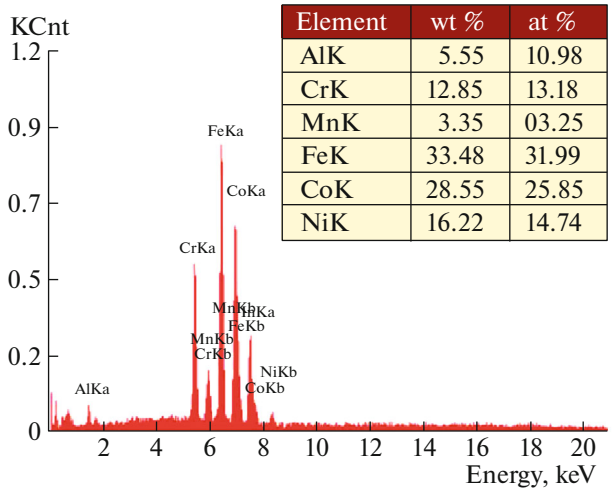

Element	wt %	at %
AlK	5.55	10.98
CrK	12.85	13.18
MnK	3.35	03.25
FeK	33.48	31.99
CoK	28.55	25.85
NiK	16.22	14.74

Fig. 3. Energy spectra obtained from the upper layer of the coating.

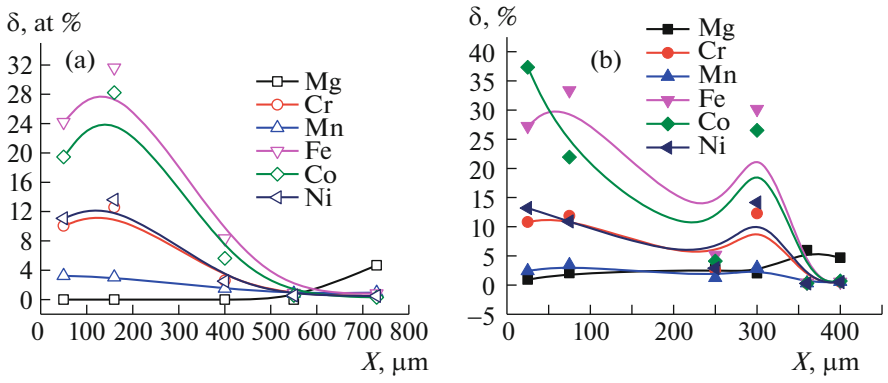

Fig. 4. Dependence of the concentration of chemical elements that form the transition layer and the substrate layer adjacent to it on the distance from the interface between the transition layer and the coating (Al is the rest); (a) and (b) two tracks of analysis.

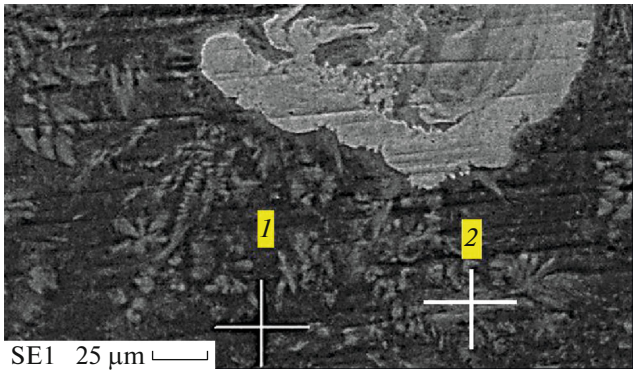

Fig. 5. Electron microscopic image of the lamellar crystallization structure of the substrate layer adjacent to the transition layer; the "+" sign indicates the sites the elemental composition at which is given in Table 4.

boundary of the transition layer. For another track (Fig. 4b), the maximum concentration of the chemical elements of the coating is revealed in the layer having a lamellar structure. These results are confirmed by the results of the data presented in Fig. 5.

Table 2. Elemental composition of different coating regions

Region	Elemental composition, at %					
	Al	Cr	Mn	Fe	Co	Ni
Upper coating layer	10.9	13.2	3.3	32.0	25.9	14.7
Middle coating layer	9.6	13.1	3.3	32.7	26.7	14.6

Table 3. Elemental composition of the coating at different distances from its surface

X, μm	Elemental composition, at %					
	Al	Cr	Mn	Fe	Co	Ni
60	7.2	13.4	3.9	33.0	27.7	14.8
380	7.2	13.2	3.4	34.0	26.9	15.3
840	5.7	13.7	3.3	34.0	28.4	14.9
1700	8	13.1	3.4	33.2	27.9	14.4
2100	9.5	13.1	3.3	32.7	26.7	14.7

Table 4. The elemental composition of the sites indicated in Fig. 5 with a "+" sign

Site	Elemental composition, at %						
	Mg	Al	Cr	Mn	Fe	Co	Ni
1	4.7	92.3	0.6	0.6	0.6	0.7	0.5
2	3.1	80.5	2.1	1.5	6.2	4.4	2.2

We performed an elemental analysis of the transition layer with a lamellar structure (Fig. 5); The quantitative results for regions 1 and 2 are given in Table 4.

The data in Table 4 suggest that a lamellar structure at the interface between the transition layer and the substrate is formed due to the doping of the coating with substrate elements.

CONCLUSIONS

Using scanning electron microscopy, we studied the structure, elemental composition, mechanical, and tribological properties of the HEA coating–5083 alloy substrate system formed by WAAM by determining its microhardness and wear resistance. The following main results have been obtained:

—Deposition of HEA on the 5083 alloy surface is accompanied by the formation of a gradient structure characterized by a regular change in microhardness, elemental, and phase composition;

—A stepwise nature of the change in the microhardness of the HEAcoating–5083 alloy substrate system was revealed;

—The formation of a transition layer up to 450 μm thick, located at the interface between the coating and the substrate, was found;

—Dopping of the coating with substrate elements (aluminum) was observed, leading to the formation of a HEA of the chemical composition Al–Mn–Fe–Cr–Co–Ni;

—The formation of a lamellar structure in the substrate layer adjacent to the coating was revealed.

FUNDING

This work was supported by the Russian Science Foundation, project no. 20-19-00452.

CONFLICT OF INTEREST

The authors declare that they have no conflicts of interest.

REFERENCES

1. Y. Zhang, Acta Mater. **188**, 435 (2020). https://doi.org/10.1016/j.Actamat.2019.12.015
2. Y. A. Alshataif, S. Sivasankaran, F. A. Al-Mufadi, A. S. Alaboodi, and H. R. Ammar, Met. Mater. Int. **26**, 1099 (2019). https://doi.org/10.1007/s12540-019-00565-z
3. D. B. Miracle and O. N. Senkov, Acta Mater. **122**, 448 (2017). https://doi.org/10.1016/j.Actamat.2016.08.081
4. W. Zhang, P. K. Liaw, and Y. Zhang, Sci. China Mater. **61** (1), 2 (2018). https://doi.org/10.1007/s40843-017-9195-8

5. K. A. Osintsev, S. V. Konovalov, V. E. Gromov, Y. F. Ivanov, and I. A. Panchenko, Mater. Lett. **312**, 131675 (2022). https://doi.org/10.1016/j.mat-let.2022.131675

6. V. E. Gromov, S. V. Konovalov, Yu. F. Ivanov, K. A. Osintsev, Yu. A. Shliarova, and A. N. Gostevskaya, Basic Probl. Mater. Sci. **2** (19), 205 (2022). https://doi.org/10.25712/ASTU.1811-1416.2022.02.008

7. B. Dong, Z. Wang, Z. Pan, O. Muránsky, C. Shen, M. Reid, B. Wu, X. Chen, and H. Li, Mater. Sci. Eng. A **802**, 140639 (2021). https://doi.org/10.1016/j.msea.2020.140639

8. Y. Zhang, X. Chen, S. Jayalakshmi, R. A. Singh, V. B. Deev, and E. S. Prusov, J. Alloys Compd. **857**, 157625 (2021). https://doi.org/10.1016/j.jallcom.2020.157625

9. T. Zhang, L. Xin, F. Wu, Xiang J. Chen, S. Jiang, Y. Huang, and S. Chen, J. Mater. Sci. Technol. **35**, 2331 (2019).

10. B. A. Gludovatz, A. Hohenwarter, D. Catoor, E. H. Chang, E. P. George, and R. O. Ritchie, Science (Washington, DC, U. S.) **345** (6201), 1153 (2014).

11. V. E. Gromov, S. V. Konovalov, Yu. F. Ivanov, and K. A. Osintsev, *Structure and Properties of High-Entropy Alloys,* Vol. 107 of *Advanced Structured Materials* (Springer, New York, 2021).

12. A. D. Pogrebnjak, A. A. Bagdasaryan, I. V. Yakushchenko, and V. M. Beresnev, Russ. Chem. Rev. **83**, 1027 (2014).

13. Y. F. Ivanov, K. A. Osintsev, V. E. Gromov, S. V. Konovalov, and I. A. Panchenko, Steel Transl. **51** (1), 27 (2021). https://doi.org/10.3103/S0967091221010046

14. K. Osintsev, S. Konovalov, V. Gromov, I. Panchenko, and Y. Ivanov, Philos. Mag. Lett. **101**, 353 (2021). https://doi.org/10.1080/09500839.2021.1936257

15. K. Osintsev, S. Konovalov, V. Gromov, I. Panchenko, and X. Chen, Mater. Today: Proc. **46**, 961 (2021). https://doi.org/10.1016/j.matpr.2021.01.079

Translated by O. Zhukova